Hydrogen production by water splitting with $Mn_{3-x}Co_xO_4$ mixed oxides thermochemical cycles: A thermodynamic analysis

María Orfila[1], María Linares[1], Raúl Molina[2], Javier Marugán[2], Juan Ángel Botas[1], Raúl Sanz[2]*

[1]Chemical, Energy and Mechanical Technology Department, [2]Chemical and Environmental Technology Department, Rey Juan Carlos University, Tulipán, s/n, 28933, Móstoles, Spain

Abstract

The high temperature required for hydrogen production by solar driven thermochemical cycles is a critical factor hindering full-scale applications. The thermochemical cycle based on Mn_3O_4/MnO redox pair is one of the most studied despite the high operating temperature required for complete de reduction step (1623-1723 K). The combination of Mn_3O_4 with Co_3O_4, a metal oxide with lower reduction temperature than Mn_3O_4 that cannot be used for hydrogen production due to thermodynamic limitations, is presented as a way to decrease significantly the energy demand of the cycle. In this work, a complete thermodynamic study of thermochemical cycles with different Mn/Co mixed oxides ($Mn_{3-x}Co_xO_4$, $0.9<x<2.7$) for hydrogen production has been performed. The study of the variation of Gibbs energy with temperature allowed to determine that the thermal reduction of the metal oxide ($Mn_{3-x}Co_xO_4$) takes place at temperatures between 1048-1173 K, which can be achieved by conventional solar concentration technologies. Unfortunately, the oxidation of the reduced metal oxide ($Mn_{3-}xCo_xO_3$) with water to produce H_2 is not feasible from a thermodynamically point of view, so a stronger oxidizing agent, as sodium hydroxide, is required. The optimum temperature for the oxidation with NaOH was found to be 1373 K, meaning that this reaction takes place at higher temperatures than those actually required for the reduction, something uncommon in thermochemical cycles for water splitting. On the other hand, after the study of the variables affecting the equilibrium like the inert gas/solid ratio, it can be concluded that in both reactions, thermal requirements can be reduced by operating at lower temperatures by means of a higher inert gas/$Mn_{3-x}Co_xO_4$ ratio. Finally, energy and exergy analysis of the system based on the solar absorption efficiency and the energy requirements predicts a solar-to-fuel efficiency and exergy efficiency of 40 % and 23 %, respectively. These values are comparable or even higher than those found in literature for other metal oxides thermochemical cycles for water splitting, thus with the advantage of working at a considerable lower temperature (1373 K).

Keywords: hydrogen production, thermochemical water splitting, manganese cobalt mixed oxides, thermodynamic analysis, energy and exergy efficiency.

1. INTRODUCTION

The current environmental problems derived from the fossil fuels consumption have motivated the research of other alternatives as energy sources. In this context, hydrogen has been widely proposed as an energy carrier for a future low carbon economy [1]. Nowadays, there are many different ways to obtain hydrogen [2] but most of them are chiefly based on fossil fuels as feedstock, mainly natural gas. A massive use of hydrogen is just reasonable if renewable sources are used for its production [3, 4]. In this context, solar driven water splitting and electrolysis of water using renewable electricity are the most promising and environmental friendly alternatives for carbon-free hydrogen production [1, 5]. Water electrolysis implies the electrochemical splitting of water into hydrogen and oxygen using a conductive electrolyte like salts, acids, bases solutions [6] or solid oxides [7]. However, a great amount of electric energy is required and this energy should come from renewable sources like wind or sun. Direct splitting of water using concentrated solar energy is the most direct and cleanest method to obtain hydrogen (reaction R1), using only the radiation coming from the sun. Unfortunately, the required temperature is very high (> 4273 K), which is far from those maximum temperatures achievable with current solar technology, around 2273 K [8].

$$H_2O \rightarrow H_2 + \frac{1}{2}O_2 \qquad \text{(R1)}$$

There are also some other problems associated to this technology, such as the separation of hydrogen and oxygen in order to avoid explosive mixtures at lower temperatures [9]. Considering all these problems, thermochemical cycles appear as an interesting technology for water splitting. A thermochemical cycle consists of two or more endo- and exothermic steps in which a metal oxide is reduced and oxidized, being the net results of all the reactions the dissociation of water into hydrogen and oxygen [10]. There are a great number of potential materials reported in literature for thermochemical cycles but

not all of them are experimentally viable [9-12]. The most important features that a potential redox material must exhibit could be summarized as follows: a) the reactions should take place at temperatures achievable with the current solar technology, b) minimum number of steps, c) fast reactions, and d) minimum energy requirements in separation processes of hydrogen from the produced streams [13, 14].

The researchers have mainly focused their efforts in two-steps thermochemical cycles because of their apparently simplicity. In these processes, a metal oxide is first thermally reduced (R2) and then oxidized with water (R3), being the overall reaction the splitting of water in ½ mol of O_2 per mol of H_2. A number of metal oxides with different pair redox, such as Fe_3O_4/FeO, ZnO/Zn, CeO_2/Ce_2O_3, etc., have been proposed and evaluated in the last 15 years [3].

$$M_xO_y \rightarrow M_xO_{y-1} + \frac{1}{2} O_2 \quad \text{(R2)}$$

$$M_xO_{y-1} + H_2O \rightarrow H_2 + M_xO_y \quad \text{(R3)}$$

However, the required temperatures for the reduction step are still very high, in the range of 1873-2273 K [15-22], so the attention has diverted to other thermochemical cycles, which require lower temperatures [23]. This is the case of using Mn_2O_3 for a three-step thermochemical cycle. Reduction of Mn_2O_3 to MnO takes place by reactions R4 and R5. Oxidation step of MnO with water is not thermodynamically favorable [23-25]. Thus, it is necessary the substitution of water with a stronger oxidizing agent, such as sodium hydroxide, which may enhance the oxidation of the reduced material during the hydrogen production reaction (R6). Consequently, a last reaction between $NaMnO_2$ and water (R7) is necessary to recover the initial manganese oxide (Mn_2O_3) and sodium hydroxide involved in the process, closing the cycle. The overall process is summarized in reactions R4-R7.

$$Mn_2O_3 \rightarrow \frac{2}{3} Mn_3O_4 + \frac{1}{6} O_2 \quad \text{(R4)}$$

$$\frac{2}{3} Mn_3O_4 \rightarrow 2\ MnO + \frac{1}{3} O_2 \quad \text{(R5)}$$

$$2\ MnO + 2\ NaOH \rightarrow 2\ NaMnO_2 + H_2 \quad \text{(R6)}$$

$$2\ NaMnO_2 + H_2O \rightarrow Mn_2O_3 + 2\ NaOH \quad \text{(R7)}$$

In this three-step thermochemical cycle, the required temperature for the reduction of Mn_3O_4 to MnO (R5) is around 1623-1723 K [23], which is still too high, and therefore leading to radiation losses and a strong impact in the efficiency of the process [26].

In order to reduce the energy requirements of this cycle, the combination of Mn_3O_4 with other metal oxides with lower temperature requirements for the reduction step, like the Co_3O_4 is proposed [27, 28]. The aim of the present work is to provide a comprehensive thermodynamic analysis of the thermochemical hydrogen production based on Mn/Co mixed oxides with different composition. To the best of our knowledge, there are no previous thermodynamic studies for the $Mn_{3-x}Co_xO_4/Mn_{3-x}Co_xO_3$ thermochemical cycles. Therefore, the thermodynamic data of the species involved in the process are not available. Consequently, in the first part of this work, the evolution of Gibbs energy with the temperature was analyzed to obtain a range of operational temperatures for hydrogen production by thermochemical water splitting. Then, the effect of using a carrier gas, to extract O_2 and H_2 form the solar reactor, was also studied. After that, the energy and exergy efficiencies of the thermochemical system were estimated by calculating the efficiency of the solar conversion into H_2 ($\eta_{Solar\ to\ Fuel}$), and into useful H_2 (ε_{exergy}). These parameters were finally compared with other metal oxides based thermochemical cycles proposed in literature for hydrogen production.

2. THERMODYNAMIC STUDY

A thermodynamic study was performed to evaluate the energy requirements, the evolution of the equilibrium temperature with the amount of carrier gas, and the efficiency of the conversion of solar energy into fuel. As different metal composition will lead to materials with different redox properties, four different Mn/Co mixed oxide materials were studied (Table 1).

Table 1. $Mn_{3-x}Co_xO_4$ materials evaluated in this study.

Chemical formula	% molar Mn	% molar Co
$Mn_{0.3}Co_{2.7}O_4$	10	90
$Mn_{0.9}Co_{2.1}O_4$	30	70
$Mn_{1.5}Co_{1.5}O_4$	50	50
$Mn_{2.1}Co_{0.9}O_4$	70	30

In a first approach, theoretical temperatures required for each reaction of the cycle were calculated from the corresponding Gibbs free energies (ΔG_r^T). It is a classic equilibrium calculation of the composition of a mixture as function of temperature, including all chemicals (reactants and products) and N_2 as inert gas. This gas would act as inert carrier for O_2 and H_2 during the real reactor operation, and its presence will affect to the partial pressure of gas compounds (O_2 and H_2) and consequently the calculation of equilibrium compositions.

ΔG_r^T was determined from the standard enthalpies and entropies of formation (ΔH_f^0 and ΔS_f^0) and the temperature dependence of the specific heat ($C_p(T)$) according to the following equations [24]:

$$\Delta G_r^T = \Delta H_r^T - T\Delta S_r^T \quad (1)$$

$$\Delta H_r^T = \Delta H_r^0 + \int_{T_0}^{T} \Delta C_p(T)dT \quad (2)$$

$$\Delta S_r^T = \Delta S_r^0 + \int_{T_0}^{T} \frac{C_p}{T}(T)dT \quad (3)$$

$$\Delta H_r^0 = \sum_{i=products} \sigma_i \left(\Delta H_f^{\emptyset}\right)_i - \sum_{i=reactants} \sigma_i \left(\Delta H_f^{\emptyset}\right)_i \quad (4)$$

$$\Delta S_r^0 = \sum_{i=products} \sigma_i \left(\Delta S_f^{\emptyset}\right)_i - \sum_{i=reactants} \sigma_i \left(\Delta S_f^{\emptyset}\right)_i \quad (5)$$

$$C_p(T) = \sum_{i=products} \sigma_i \left(C_p(T)\right)_i - \sum_{i=reactants} \sigma_i \left(C_p(T)\right)_i \quad (6)$$

$$\left(C_p(T)\right)_i = A + B \cdot 10^{-3} \cdot T + C \cdot 10^5 \cdot T^{-2} + D \cdot 10^6 \cdot T^2 \quad (7)$$

where σ_i represents the stoichiometric coefficients according to the reactions of the thermochemical cycle ($\sigma_i > 0$ for the products and $\sigma_i < 0$ for the reactants). The temperature dependence equation of specific heat at constant pressure (C_p) and the values for the standard enthalpies of formation (ΔH_f^0), standard entropies of formation (ΔS_f^0), and the derived standard Gibbs energies of formation (ΔG_f^0) of O_2, H_2, NaOH and H_2O were obtained from the HSC Chemistry 6.0 software from ©Outotec Research Oy (shown in Tables S1 and S2 of supplementary material). The data for the mixed Mn/Co oxides

were determined using the Neumann-Kopp Rule (NKR) for mixed oxides, following the procedure for complex mixed oxides described elsewhere [29, 30], and from data for pure manganese and cobalt oxides (Mn_2O_3, Mn_3O_4 and Co_3O_4), obtained also from the HSC Chemistry 6.0 software.

2.1. Equilibrium calculations

Equilibrium compositions as a function of the temperature have been calculated following standard thermodynamic methods [25]. Equilibrium constants (K_p) of the reactions at constant pressure as a function of temperature were calculated according to equation 8, obtained as explained above.

$$K_p = exp\left(\frac{-\Delta G_r^T}{RT}\right) = exp\left(\frac{-\Delta H_r^T + T\Delta S_r^T}{RT}\right) \quad (8)$$

Once calculated K_p, the evolution of the mixture of reagents and products as a function of the temperature at a constant pressure (P_T) has been calculated. Firstly, it is necessary to calculate the partial pressure and the gas composition at equilibrium ($P_{O_2}^{eq}$ and $y_{O_2}^{eq}$ or $P_{H_2}^{eq}$ and $y_{H_2}^{eq}$ respectively) as follows:

1) *Reduction of $Mn_{3-x}Co_xO_4$:*

$$P_{o_2}^{eq} = K_p^{1/\sigma_{O_2}} \quad (9)$$

$$y_{O_2}^{eq} = \frac{P_{O_2}^{eq}}{P_T} \quad (10)$$

2) *Oxidation of $Mn_{3-x}Co_xO_3$ with NaOH:*

$$P_{H_2}^{eq} = K_p^{1/\sigma_{H_2}} \quad (11)$$

$$y_{H_2}^{eq} = \frac{P_{H_2}^{eq}}{P_T} \quad (12)$$

The molar amount of O_2 ($N_{O_2}^{rq}$) or H_2 ($N_{H_2}^{rq}$) that have appeared through the reaction are obtained from the difference between the initial amount of O_2 ($N_{O_2}^{0}$) or H_2 ($N_{H_2}^{0}$) and their equilibrium amount, ($N_{O_2}^{eq}$) or ($N_{H_2}^{eq}$). It should be pointed that composition of gas phase, $N_{O_2}^{eq}$ or $N_{H_2}^{eq}$, is affected by the presence of the inert gas (N_2). For that reason, taking into account the partial pressure of N_2 and O_2 as function of total pressure and gas molar fraction of each compound, and the ideal gas law, $N_{O_2}^{rq}$ and $N_{H_2}^{rq}$ can be calculated according to equations 13-16, where N_{N_2} is the molar amount of N_2 in the system.

1) *Reduction of $Mn_{3-x}Co_xO_4$:*

$$N_{O_2}^{eq} = N_{N_2} \cdot \frac{y_{O_2}^{eq}}{1-y_{O_2}^{eq}} \quad (13)$$

$$N_{O_2}^{rq} = {N_{O_2}}^{eq} - {N_{O_2}}^{0} \quad (14)$$

2) *Oxidation of $Mn_{3-x}Co_xO_3$ with NaOH:*

$$N_{H_2}^{eq} = N_{N_2} \cdot \frac{y_{H_2}^{eq}}{1-(y_{H_2}^{eq})} \quad (15)$$

$$N_{H_2}^{rq} = {N_{H_2}}^{eq} - {N_{H_2}}^{0} \quad (16)$$

Finally, the molar amount of the solid phases at the equilibrium has been computed from the produced O_2 or H_2 according to the stoichiometry of the reactions of the thermochemical cycle (equations 17-20):

1) *Reduction of $Mn_{3-x}Co_xO_4$:*

$$N_{reactant\,(s)} = N_{reactant}^{0} + \frac{\sigma_{reactant}}{\sigma_{O_2}} \cdot N_{O_2}^{rq} \quad (17)$$

$$N_{product\ (s)} = N^0_{product} + \frac{\sigma_{product}}{\sigma_{O_2}} \cdot N^{rq}_{O_2} \quad (18)$$

Where reactant is $Mn_{3-x}Co_xO_4$ and product is $Mn_{3-x}Co_xO_3$.

2) *Oxidation of $Mn_{3-x}Co_xO_3$ with NaOH:*

$$N_{reactants\ (s)} = N^0_{reactants} + \frac{\sigma_{reactants}}{\sigma_{H_2}} \cdot N^{rq}_{H_2} \quad (19)$$

$$N_{product\ (s)} = N^0_{product} + \frac{\sigma_{product}}{\sigma_{H_2}} \cdot N^{rq}_{H_2} \quad (20)$$

Where reactants are NaOH and $Mn_{3-x}Co_xO_3$, and product is $Na_2Mn_{3-x}Co_xO_5$.

2.2. Energy and exergy evaluation

A comprehensive evaluation of a thermodynamic system needs both energy and exergy analyses. Therefore, in this section, simplified energy and exergy analyses of the Mn/Co mixed oxide based cycles are presented, assuming the process schematically depicted in Figure 1. The objective of this study is to compare the results obtained with the mixed oxides used in this work ($Mn_{3-x}Co_xO_4$) with other materials previously evaluated in literature for the same application [31].

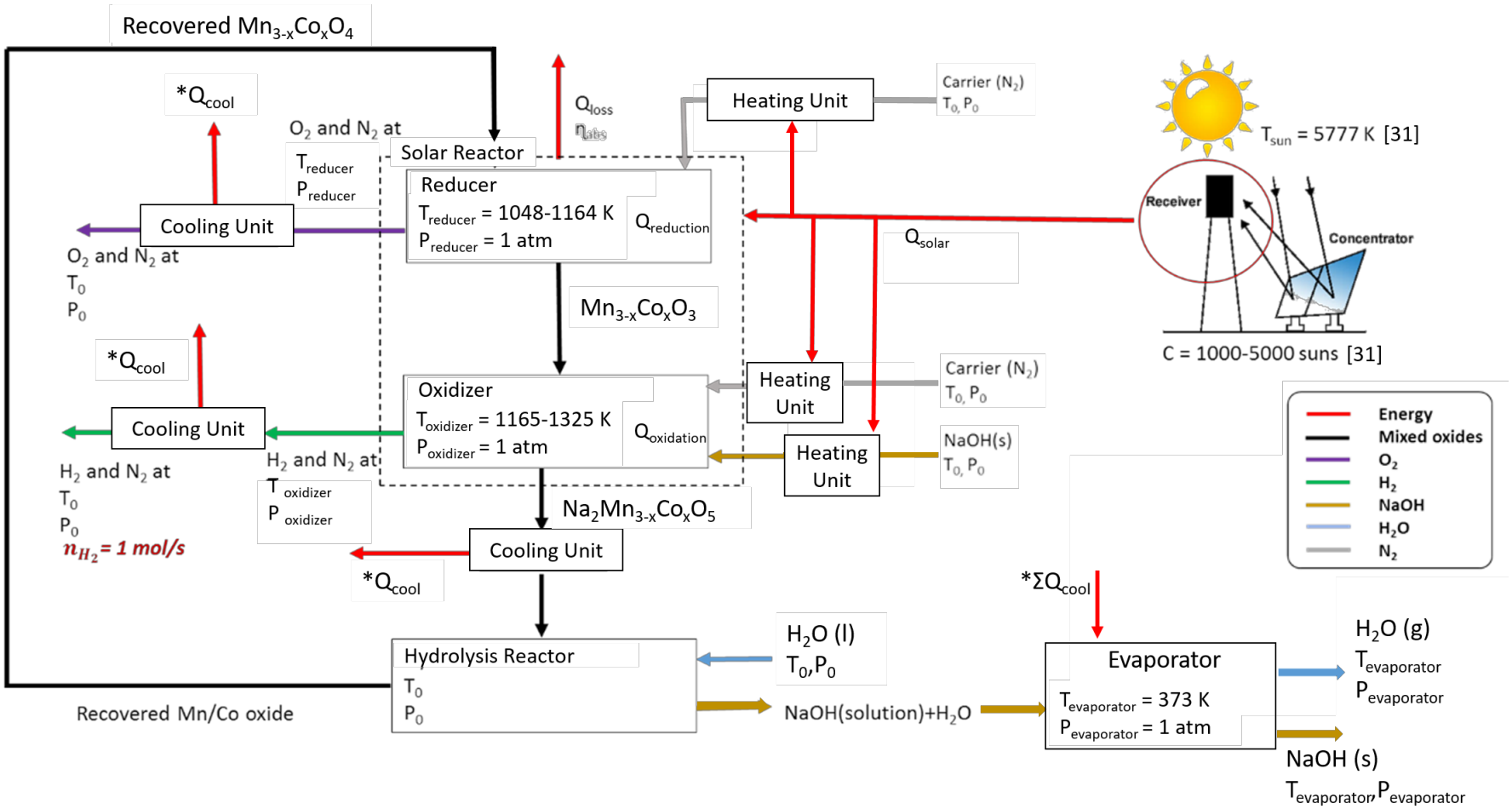

Figure 1. Flow diagram for H_2 production via three-step thermochemical water splitting cycle based on Mn/Co mixed oxides with the associated input and output heating rates of the process.

The thermochemical process here proposed consists of a solar concentrator, a receiver, a solar reactor in which reduction of $Mn_{3-x}Co_xO_4$ and oxidation of $Mn_{3-x}Co_xO_3$ would take place, cooling units for the produced O_2, H_2, and the resultant $Na_2Mn_{3-x}Co_xO_4$, heating units for the carrier gas and NaOH and finally a hydrolysis reactor to recover the initial $Mn_{3-x}Co_xO_4$ mixed oxide (Figure 1). Temperature and pressure of 298 K and 1 bar were fixed as ambient conditions (T_0 and P_0), respectively. The complete cycle was assumed to occur at steady-state, being neglected viscous losses, kinetic and potential energies. The cycle was normalized to a production of 1 mol/s of H_2.

The solar reactor was considered as perfectly insulated, blackbody receiver, so the absorption efficiency is given by equation 21 [17, 32].

$$\eta_{abs_i} = \frac{Q_{solar\ reactor}}{Q_{solar}} = 1 - \frac{\sigma \cdot T_i^4}{I \cdot C} \tag{21}$$

where Q_{solar} is the total solar heat rate input to the reactor; $Q_{solar\ reactor}$ is the total heat needed by the reactions to take place (reduction and oxidation) as a function of the required temperature (T_i), σ is the Stefan-Boltzmann constant ($5.67 \cdot 10^{-11}$ kW/m^2·K^4); T_i is the required temperature ($T_{reduction}$ or $T_{oxidation}$) in Kelvin; I is the direct-normal solar irradiation taken as 1 kW·m^2; and C is the concentration ratio which is defined as the solar radiative flux normalized to 1 kW/m^2 and it is usually expressed in "suns" units.

The initial Mn/Co oxide ($Mn_{3-x}Co_xO_4$) was assumed to enter inside the solar reactor and be reduced at a total pressure of 1 atm. The energy necessary for the reduction reaction is given by equation 22 [33].

$$Q_{reduction} = n_{H_2} \cdot T_{reduction} \cdot \Delta S|_{Reactants@T_0P_0 \rightarrow Products@T_{reduction}P_0} \tag{22}$$

The released O_2 was continuously removed with the inert carrier gas (N_2). The energy necessary to heat the nitrogen to the required temperature is described by equation 23.

$$Q_{heating\ N_2} = n_{N_2} \cdot \Delta H|_{N_2@T_0 \rightarrow T_{reduction}} \quad (23)$$

Thus, the required heat for the reduction step can be summarized as expressed in equation 24.

$$Q_{net\ reduction} = Q_{reduction} + Q_{heating\ N_2} \quad (24)$$

The reduced material ($Mn_{3-x}Co_xO_3$) was mixed with NaOH obtaining $Na_2Mn_{3-x}Co_xO_5$ during the oxidation step, assuming an adiabatic and isobaric operation. The energy required to perform the reaction with NaOH is described by equation 25.

$$Q_{oxidation} = n_{H_2} \cdot T_{oxidation} \cdot \Delta S|_{Reactants@T_0P_0 \rightarrow Products@T_{oxidation}P_0} \quad (25)$$

In this case it should be mentioned that one of the reactants, NaOH, suffers a state change at 591 K, being necessary to include in this equation the latent fusion heat ($\lambda_{NaOH\ fusion}$).

Additionally, it is necessary to heat the N_2 carrier before feeding to the oxidation step, as is indicated in equation 26.

$$Q_{heating\ N_2} = n_{N_2} \cdot \Delta H|_{N_2@T_0 \rightarrow T_{oxidation}} \quad (26)$$

Thus, the required heat for the oxidation step can be summarized as expressed in equation 27.

$$Q_{net\ oxidation} = Q_{oxidation} + Q_{heating\ N_2} \quad (27)$$

Taking this into account, the required energy ($Q_{solar\ reactor}$) is given by equation 28.

$$Q_{solar\ reactor} = Q_{net\ reduction} + Q_{net\ oxidation} \quad (28)$$

So, the total solar heat rate (Q_{solar}) can be calculated combining equations 21 and 28 as expressed in equation 29. Each step (reduction and oxidation) occurring in the solar reactor could take place at different temperature. The higher the temperature, the lower

the η_{abs} and consequently higher Q_{solar} from the sun would be necessary. As both processes occurs in the same solar receiver and with the same solar irradiation, the worst case scenario will be taken for this study. This means that Q_{solar} will be calculated taking into account the higher temperature and consequently the minimum η_{abs}, between both reduction and oxidation steps.

$$Q_{solar} = \frac{Q_{net\,reduction}}{\eta_{abs_{reduction}}} + \frac{Q_{net\,oxidation}}{\eta_{abs_{oxidation}}} = \frac{Q_{reduction}+Q_{heatingN_2}}{\eta_{abs_{reduction}}} + \frac{Q_{oxidation}+Q_{heating\,NaOH+N_2}}{\eta_{abs_{oxidation}}} \cong \frac{Q_{reduction}+Q_{heatingN_2}+Q_{oxidation}+Q_{heating\,NaOH+N_2}}{minimium\,(\eta_{abs_{reduction}},\eta_{abs_{oxidation}})} = \frac{Q_{reduction}+Q_{heatingN_2}+Q_{oxidation}+Q_{heating\,NaOH+N_2}}{\eta_{abs}} \quad (29)$$

Finally, the heat loss due to the re-radiation from the reactor to the environment can be described as equation 30.

$$Q_{loss} = Q_{solar}(1-\eta_{abs}) \quad (30)$$

The O_2 and N_2 stream exiting from the reduction step is cooled down to ambient temperature so the heat rejected in the cooling unit is calculated by equation 31.

$$Q_{cool\,O_2,N_2} = n_{O_2}\cdot \Delta H|_{O_2@T_{reduction}\rightarrow T_0} + n_{N_2}\cdot \Delta H|_{N_2@T_{reduction}\rightarrow T_0} \quad (31)$$

In the same way, the gas mixture (H_2/N_2) from the oxidation step goes also through a cooling unit reaching ambient temperature. The heat rejected in this case is given by equation 32.

$$Q_{cool\,H_2,N_2} = n_{H_2}\cdot \Delta H|_{H_2@T_{oxidation}\rightarrow T_0} + n_{N_2}\cdot \Delta H|_{N_2@T_{oxidation}\rightarrow T_0} \quad (32)$$

Hydrolysis at ambient temperature has been assumed in order to obtain a resultant solution of NaOH in liquid water. Thus, it is necessary to cool down the recovered oxide ($Na_2Mn_{3-x}Co_xO_5$) before feeding to the hydrolysis reactor as given by equation 33.

$$Q_{cool\ Na_2Mn_{3-x}Co_xO_5} = n_{Na_2Mn_{3-x}Co_xO_5} \cdot \Delta H|_{NNa_2Mn_{3-x}Co_xO_5, T_{oxidation} \rightarrow T_0} \quad (33)$$

The heat necessary to recover the NaOH in the evaporator is given by equation 34.

$$Q_{evaporator} = n_{H_2O} \cdot \Delta H|_{H_2O@T_0 \rightarrow T_{evaporation H_2O}} + n_{H_2O} \cdot \lambda_{H_2O evaporation} + n_{NaOH} \cdot \Delta H|_{NaOH@T_0 \rightarrow T_{evaporation H_2O}} \quad (34)$$

As the evaporation step has been postulated as one of the main energy terms of the system [34], this work evaluate the possible use of the heat recovered from the cooling units ($\sum Q_{cool}$) for evaporation and recovering of the NaOH.

The solar to fuel efficiency is a parameter used to compare the potential heat production from the hydrogen with the solar heat inputs, and it is determined by equation 35 [32].

$$\eta_{solar\ to\ fuel} = \frac{n_{H_2} \cdot HHV_{H_2}}{Q_{solar} + Q_{evaporator}} \quad (35)$$

where HHV_{H2} is the hydrogen higher heating value (286 kJ/mol) [2].

On the other hand, the exergy associated to Q_{solar} is described by ψ_{solar}, which is the exergy associated with undiluted thermal radiation from the sun determined in equation 36 [35].

$$\psi_{solar} = Q_{solar} \cdot \left(1 - \frac{4}{3} \cdot \frac{T_0}{T_{sun}} + \frac{1}{3} \cdot \left(\frac{T_0}{T_{sun}}\right)^4\right) \quad (36)$$

where T_{sun} has a value of 5777 K, which is considered the effective temperature of the Sun.

The exergy of the evaporator must be also taken into account. This exergy can be described as equation 37 [32],

$$\psi_{evaporator} = n_{H_2O} \cdot \Delta\psi_{flow}\Big|_{H_2O(l)@T_0 \rightarrow H_2O(v)@T_{evsaporation}} +$$

$$+ n_{NaOH} \cdot \Delta\psi_{flow}\Big|_{NaOH@T_0 \rightarrow T_{evaporationH_2O}} \quad (37)$$

Finally, exergy efficiency was calculated as a relation between the input energy and the potential electricity generation. This potential energy was calculated assuming that H_2 is used as fuel in a fuel cell for electricity production with an efficiency of 65 %, which is a value used for similar studies in literature [31]. This efficiency is given by equation 38.

$$\varepsilon_{exergy} = \frac{0.65 \cdot n_{H_2} \cdot \psi_{ch,H_2}}{\psi_{solar} + \psi_{evaporator}} \quad (38)$$

where ψ_{ch,H_2} is the chemical exergy of the hydrogen that has an estimated value of 235.2 kJ/mol [32, 36].

3. RESULTS AND DISCUSSION

3.1. Feasibility of the reactions

The evaluation of novel redox materials, such as $Mn_{3-x}Co_xO_4$, for thermochemical hydrogen production should be theoretically analyzed to ensure the feasibility of the process. Four $Mn_{3-x}Co_xO_4$ (x = 0.9, 1.5, 2.1, 2.7) mixed oxides were studied as it was indicated in Table 1. A three-step thermochemical cycle has been assumed for these materials, according to the original Mn_2O_3/MnO cycle. However, the first approach was to evaluate the possibility of a simpler two-step thermochemical cycle, avoiding the use of NaOH as oxidizing agent. According to this, it can be assumed that the cycle of the

mixed oxides proceeds through the reduction of $Mn_{3-x}Co_xO_4$ in an endothermic reaction at high temperature (reaction R8), and the subsequent oxidation with water to obtain hydrogen and the initial material (reaction R9):

$$Mn_{3-x}Co_xO_4 \rightarrow Mn_{3-x}Co_xO_3 + \frac{1}{2} O_2 \quad \text{(R8)}$$

$$Mn_{3-x}Co_xO_3 + H_2O \rightarrow Mn_{3-x}Co_xO_4 + H_2 \quad \text{(R9)}$$

The variation with the temperature of the theoretical Gibbs energies for the reduction step of each Mn/Co mixed oxide are shown in Figure 2a. These results show that thermal reduction of the Mn-Co mixed oxides takes place at temperatures between 1048 K and 1164 K, depending on the amount of manganese present in the mixed oxide. The higher the proportion of manganese (70 % mol, sample $Mn_{2.1}Co_{0.9}O_4$) the higher temperature is required. This result is in agreement with the higher reduction temperature of the Mn_2O_3/MnO redox pair, 1723 K [25, 37], in comparison with that of Co_3O_4, 1118 K (Supplementary Material, Figure S1a). From a theoretical point of view, this important decrease in the temperature required for the reduction step could lead to a higher efficiency of the solar production system (equation 21), and consequently to an increase in the global efficiency of the cycle according to equations 35 and 37.

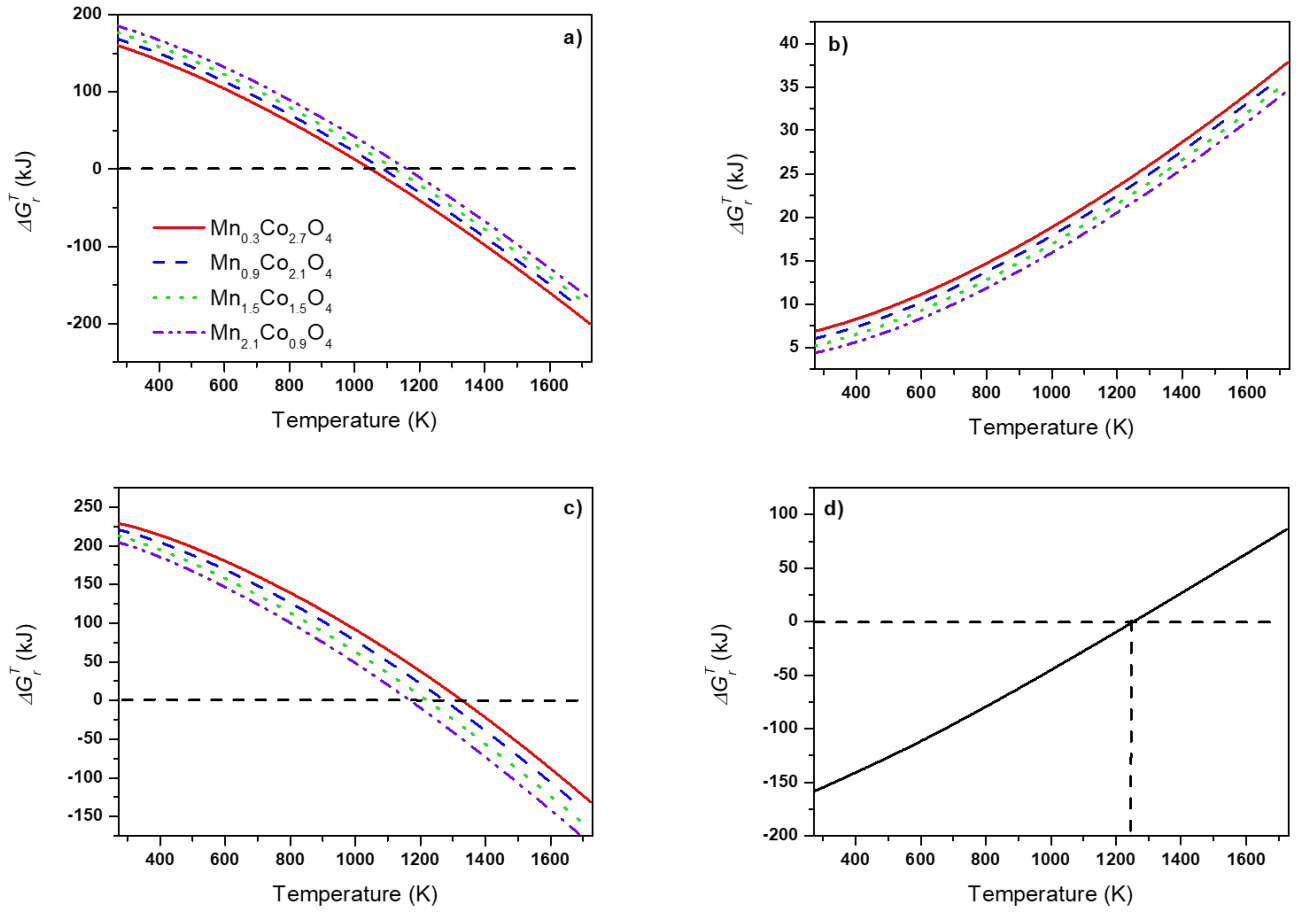

Figure 2. ΔG_r^T vs Temperature for: a) thermal reduction, b) oxidation with water, c) oxidation with NaOH, and d) hydrolysis of the resultant Na-Mn-Co-oxide material.

Once calculated the required temperature for the reduction reaction, the viability of the oxidation with water (reaction R9) was studied. As it can be seen in Figure 2b, the oxidation of $Mn_{3-x}Co_xO_3$ with water is not feasible in the range of temperatures under study. The same behavior was obtained for the reduced MnO and CoO pure materials (Supplementary Material, Figure S1b). The reaction between water and a reduced oxide is thermodynamically possible only if the Gibbs energy of the metal oxide redox pair is greater than the corresponding for the water reduction. Based on the diagram shown in

Figure S2, it can be concluded that direct water-splitting is not possible with MnO or CoO, so neither with a mixture of them.

The alternative consists of using a more powerful oxidizing compound such as the sodium hydroxide to reoxidized the reduced oxide with hydrogen production (reaction R10), according to results in Figure S2.

$$Mn_{3-x}Co_xO_3 + 2\ NaOH \rightarrow Na_2Mn_{3-x}Co_xO_5 + H_2 \quad (R10)$$

As it can be seen in Figure 2c, the reaction with NaOH is an endothermic process, which is possible for all the studied materials. It takes place at temperatures in the range of ca. 1165-1325 K, depending on the Mn/Co proportion. The required temperature for the process decreases with increasing the quantity of manganese present in the material. This could be explained because CoO does not react with NaOH (Figure S1c, supplementary material), so its presence could partially inhibit the oxidation steps.

In this case, a third reaction (hydrolysis of $Na_2Mn_{3-x}Co_xO_5$, reaction R11) should be added in order to close the thermochemical cycle, and obtain the decomposition of water into O_2 and H_2 as net result.

$$Na_2Mn_{3-x}Co_xO_5 + H_2O \rightarrow Mn_{3-x}Co_xO_4 + 2\ NaOH \quad (R11)$$

The evolution of ΔG_r^T with temperature was identical for all the starting materials (Figure 2d). The results show that this last step of the thermochemical cycle is thermodynamically feasible even at ambient temperature for all the studied materials, although at this temperature the kinetics would be very slow.

Table 2 summarizes the temperatures required for reduction and oxidation steps of each material. It is remarkable that the oxidation reaction with NaOH requires higher temperatures than thermal reduction, being the most energy demanding step. On the other

hand, the heat losses derived from the high temperatures used and the gap between the temperature for the reduction and oxidation steps are the main factors reducing the exergy efficiency [36]. Thus, it is desirable that the temperature at which both steps take place are as much similar as possible. It is noteworthy that material $Mn_{2.1}Co_{0.9}O_4$ shows a negligible gap between both reduction and oxidation temperatures (1164 and 1165 K, respectively), being the most promising material at this point of the study.

Table 2. Temperature requirements for thermal reduction and oxidation with NaOH (R8 and R10).

Starting material	% Mn	% Co	$T_{reduction}$ (K)	$T_{oxidation}$ (K)
$Mn_{0.3}Co_{2,7}O_4$	10	90	1048	1325
$Mn_{0.9}Co_{2.1}O_4$	30	70	1090	1268
$Mn_{1.5}Co_{1.5}O_4$	50	50	1124	1221
$Mn_{2.1}Co_{0.9}O_4$	70	30	1164	1165

Summarizing these results, it can be concluded that the presence of Co has a positive effect, decreasing the thermal reduction temperature required for the pure Mn_2O_3/MnO cycle, from 1723 K [26] to 1048-1164 K. However, a high proportion in Co affects negatively the oxidation step, being necessary to reach a compromise on the amount of Co present in the manganese-cobalt mixed oxides. Taking these results into account, it can be confirmed that a complete thermochemical cycle for hydrogen production based on $Mn_{3-x}Co_xO_4$ materials is possible, with maximum operating temperatures of 1325 K, being very attractive for a full-scale application. Finally, among all the studied materials, $Mn_{2.1}Co_{0.9}O_4$ presents a negligible gap between both reduction and oxidation

temperatures which could lead to a higher efficiency of the system, being the most promising material of all the studied ones.

3.2. Equilibrium calculation

The ΔG_r^T is a parameter that shows the temperature at which reactions become spontaneous. However, it doesn't mean that those reactions should proceed to 100 % of extent. Thus, it is necessary to combine the evaluation of ΔG_r^T with a study of the equilibrium composition of each reaction as a function of temperature. Figure 4 shows the evolution of the composition with the temperature on the thermodynamic equilibrium of the reduction and oxidation steps of the Mn/Co mixed oxides based thermochemical cycles, while Table 3 summarizes the required temperatures to achieve a conversion of 100 % (T^{final}). Table 3 also includes data corresponding to T^{eq} ($\Delta G_r^T = 0$), calculated by thermodynamic study above commented (Table 2), for both reduction and oxidation steps.

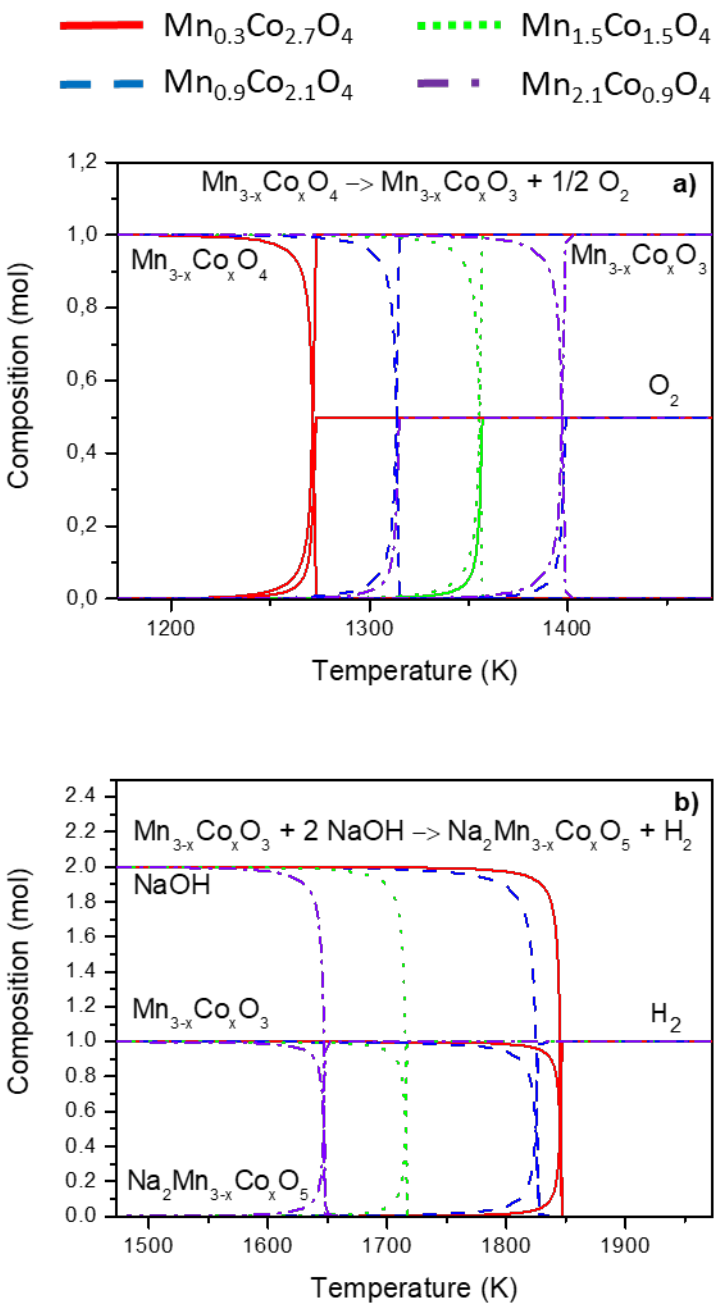

Figure 3. Equilibrium compositions for: a) reduction, and b) oxidation steps of the thermochemical cycle with Mn/Co mixed oxides (P = 1 bar and 1 mol $Mn_{3-x}Co_xO_4$).

Table 3. Required temperatures to achieve a conversion of 100 % (T^{final}) and for $\Delta G_r^T = 0$ (T^{eq}).

Starting material	Reduction Step		Starting material	Oxidation Step	
	T^{eq} (K)	T^{final} (K)		T^{eq} (K)	T^{final} (K)
$Mn_{0.3}Co_{2.7}O_4$	1048	1273	$Mn_{0.3}Co_{2.7}O_3$	1325	1846
$Mn_{0.9}Co_{2.1}O_4$	1090	1315	$Mn_{0.9}Co_{2.1}O_3$	1268	1828
$Mn_{1.5}Co_{1.5}O_4$	1124	1357	$Mn_{1.5}Co_{1.5}O_3$	1221	1717
$Mn_{2.1}Co_{0.9}O_4$	1164	1399	$Mn_{2.1}Co_{0.9}O_3$	1165	1648

As it can be seen in Figure 3 and Table 3, the required temperatures to achieve a total conversion (T^{final}) are much higher than those predicted by the thermodynamic study (T^{eq}), ca. 230 K higher for the reduction, and 515 K for the oxidation. Thus, oxidation of $Mn_{2.1}Co_{0.9}O_3$ requires a final temperature of 1648 K to obtain a complete oxidation. In the case of the material $Mn_{0.3}Co_{2.7}O_3$, a temperature as high as 1846 K is required.

From a practical point of view, it is necessary to use an inert gas as a carrier for hydrogen and oxygen generated in the different steps of the cycle, as it is exposed in the real process simulated in Figure 1. In the equilibrium calculations the presence of N_2 in the gas phase will decrease the partial pressure of O_2 and H_2, and consequently modify the overall equilibrium composition with temperature [25, 29]. Thus, the influence of the N_2 was evaluated by comparing the system with different N_2/mixed oxide molar ratio with the basic case in absence of N_2 showed in Figure 3. Figure 4 shows the results for reduction and oxidation steps of $Mn_{2.1}Co_{0.9}O_4$/$Mn_{2.1}Co_{0.9}O_3$ cycle, as example, while a summary of the changes in T^{final} for all Mn/Co materials as function of N_2/mixed oxides is shown in Tables 4 and 5, respectively. The graphs for the rest of materials are shown in Figures S3-S5 from Supplementary Material.

The effect of using N_2 in both reactions is quite similar, leading to lower operational temperatures when increasing the N_2 proportion. This fact is related to the decrease on the partial pressures of oxygen and hydrogen, and thus, the equilibrium is shifted to the formation of products following *Le Châtelier*'s principle. A decreasing of the temperatures required for reduction and oxidation was estimated for all the materials when increasing the amount of N_2 from 0.1 to 3 mol per mol of mixed oxide (Tables 4 and 5). This effect is higher in the case of the oxidation reaction due to the higher value of the stoichiometric coefficient of the hydrogen in reaction R10 vs oxygen in reaction R8 (Table 5). Moreover, the higher the amount of Mn presented in the mixed oxides, the lower the difference between both temperatures.

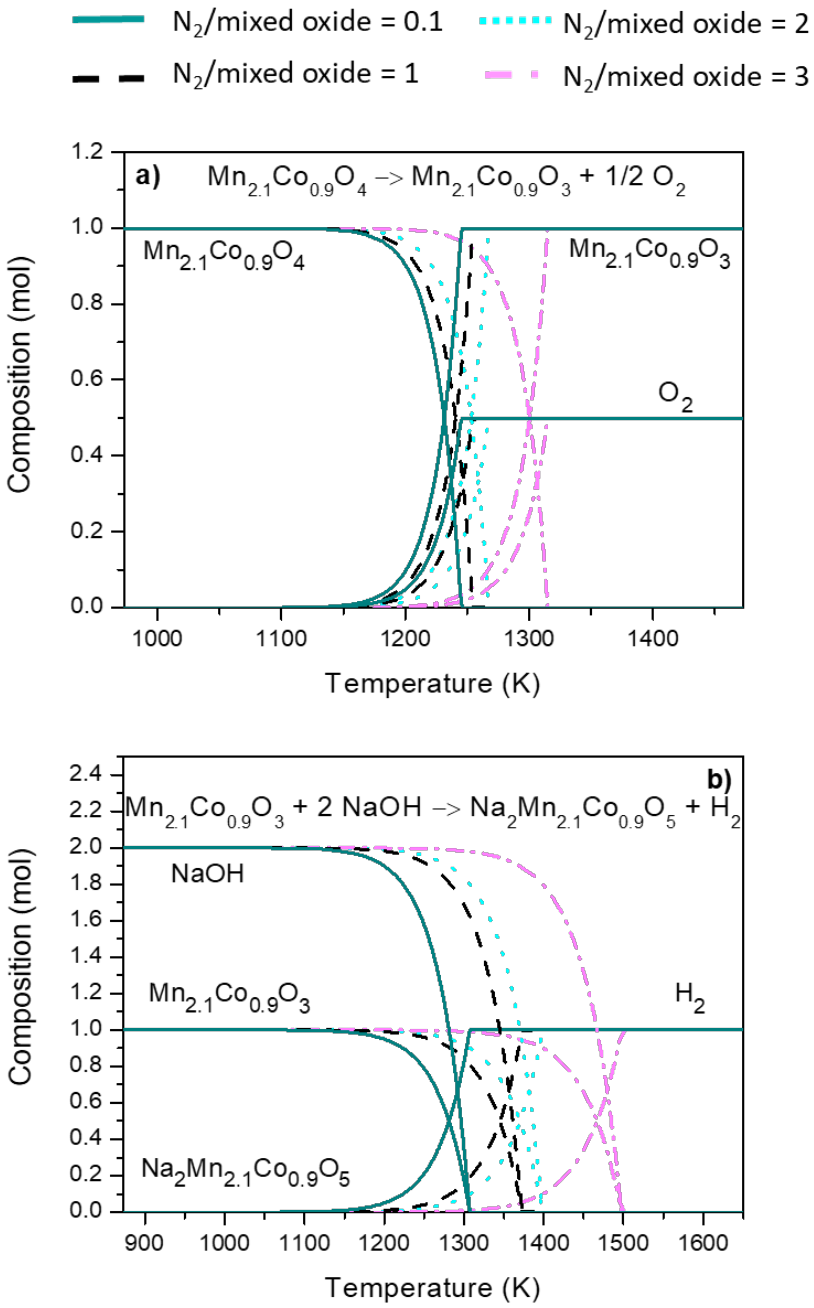

Figure 4. Equilibrium compositions for: a) reduction, and b) oxidation steps of the thermochemical cycle with $Mn_{2.1}Co_{0.9}O_4$ as function of N_2/mixed oxide proportion (P = 1 bar, 1 mol of $Mn_{2.1}Co_{0.9}O_4$).

Table 4. Temperature requirements for complete thermal reduction of $Mn_{3-x}Co_xO_4$ at different N_2/mixed oxide molar ratio.

Starting Material	T^{eq} (K)	T^{final} (K)			
		N_2/mixed oxide = 0.1	N_2/mixed oxide = 1	N_2/mixed oxide = 2	N_2/mixed oxide = 3
$Mn_{0.3}Co_{2.7}O_4$	1048	1186	1148	1138	1128
$Mn_{0.9}Co_{2.1}O_4$	1090	1235	1188	1175	1168
$Mn_{1.5}Co_{1.5}O_4$	1124	1273	1226	1213	1203
$Mn_{2.1}Co_{0.9}O_4$	1164	1323	1268	1253	1246

Table 5. Temperature requirements for complete oxidation of $Mn_{3-x}Co_xO_3$ with NaOH at different N_2/mixed oxide molar ratio.

Starting Material	T^{eq} (K)	T^{final} (K)			
		N_2/mixed oxide = 0.1	N_2/mixed oxide = 1	N_2/mixed oxide = 2	N_2/mixed oxide = 3
$Mn_{0.3}Co_{2.7}O_3$	1325	1723	1598	1573	1534
$Mn_{0.9}Co_{2.1}O_3$	1268	1643	1527	1498	1472
$Mn_{1.5}Co_{1.5}O_3$	1221	1573	1468	1433	1411
$Mn_{2.1}Co_{0.9}O_3$	1165	1503	1398	1373	1352

Summarizing, it can be concluded that the presence of a small amount of Co in the mixed oxides decreases the reduction temperature as compare to the pure Mn_2O_3/MnO thermochemical cycle. However, the increase in the proportion of Co produces a shift towards higher oxidation temperatures, being necessary to reach a compromise between both temperatures, as the gap between them is a critical factor for the viability of the

process, in terms of efficiency [31]. Furthermore, taking into account the influence of the amount of inert gas introduced into the system, it is clear that it is more favorable to work with high N_2/mixed oxides molar ratios, which can be extrapolated to work in the presence of a certain flow of inert gas to carry out the O_2 and H_2 from the reactor.

3.3. Energy and Exergy evaluation

Energy and exergy analysis of the thermochemical cycle proposed have been developed taking into account the results above obtained, which allow the formulation of the following assumptions:

i) Both reduction and oxidation reactions would occur adiabatically and isobarically, at the temperature required for the reaction. No further losses between steps are taking into account.

ii) The oxidation of the reduced Mn/Co materials ($Mn_{3-x}Co_xO_3$) with NaOH is the step with higher temperature requirements. Thus, the oxidizer with its temperature requirements and η_{abs}, will be used for the analysis of the solar absorption efficiency with temperature.

iii) Concentration ratio (C) is critical in this study, as the temperatures that can be reached in solar thermal facilities for a constant Q_{solar} are directly related with this parameter. Although a value of 5000 suns is commonly found in literature for this kind of evaluations [33, 35], the influence of this parameter will be studied in this work.

iv) The final recovering step (hydrolysis of $Na_2Mn_{3-x}Co_xO_5$) proceeds at ambient temperature (T_0) and pressure (P_0), obtaining the starting mixed oxide as a solution of NaOH in liquid water.

3.3.1 Solar absorption efficiency

Figure 5 shows the evolution of the solar absorption efficiency with the temperature in the oxidation step for the different mixed oxides studied. C values between 1000 and 5000 suns have been used. Due to the differences between the temperature predicted by the Gibbs free energy (T^{eq}) and the required temperature to achieve a total conversion (T^{final}), Tables 4 and 5, a comparison of results at both temperatures is included.

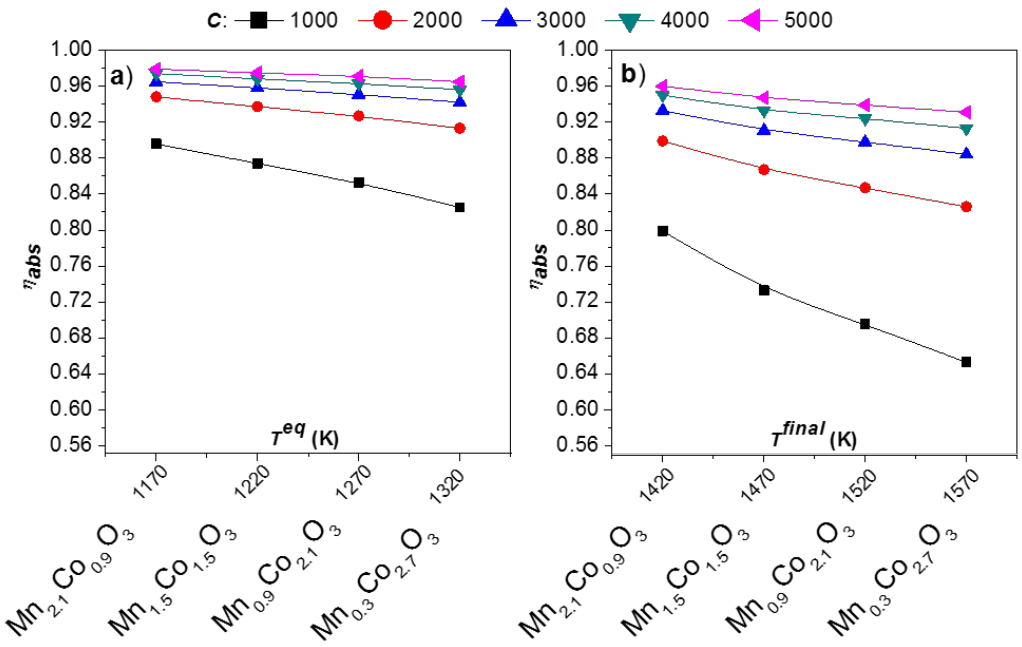

Figure 5. Solar absorption efficiency of the oxidation step of the $Mn_{3-x}Co_xO_4/Mn_{3-x}Co_xO_3$ according to: a) T^{eq}, and b) T^{final}, for N_2/mixed oxide = 2.

A decrease in the efficiency was observed for thermochemical cycles performed with materials with lower Mn-content as they required higher temperatures for the oxidation. This is consequence of the high re-radiative losses associated with an increasing $T_{oxidation}$ in those materials (equations 21 and 30). Comparison of results at T^{eq} and T^{final} (Figures 5a and 5b, respectively) reveal a similar behavior. The η_{abs} decreases when consider T^{final} for a complete oxidation of the material, instead of T^{eq} for $\Delta G_r^T = 0$, due to the difference

between both values. It is especially remarkable at C = 1000-2000 suns, although $Mn_{2.1}Co_{0.9}O_3$ exhibited the higher values of η_{abs}, achieving efficiencies higher than 90 % with concentration ratios in the solar facility of 2000 suns (in case of T^{eq}) or 3000 suns (for T^{final}).

Regarding the influence of C, the effect is more remarkable as lower Mn content in the materials. Nevertheless, the influence is higher at lower C (1000-2000 suns) being the difference lower than 3 % for $C \geq 3000$ suns.

3.3.2. Solar heat input

Energy requirements in the solar reactor are influenced by both the enthalpy of the reactions and the preheating of the N_2 used as carrier. Actually, this last variable has a critical influence in the T^{eq} and T^{final} of the reaction, as higher N_2/mixed oxide ratio decreases both temperatures. But, at the same time, the higher the N_2/mixed oxide ratio, the higher the energy requirements to preheat de inert gas stream. The overall influence of the N_2/mixed oxide ratio due to this two opposite effects is evaluated in Figure 6, by calculation of the required solar heat input (calculated as described in equation 29) for different values of C.

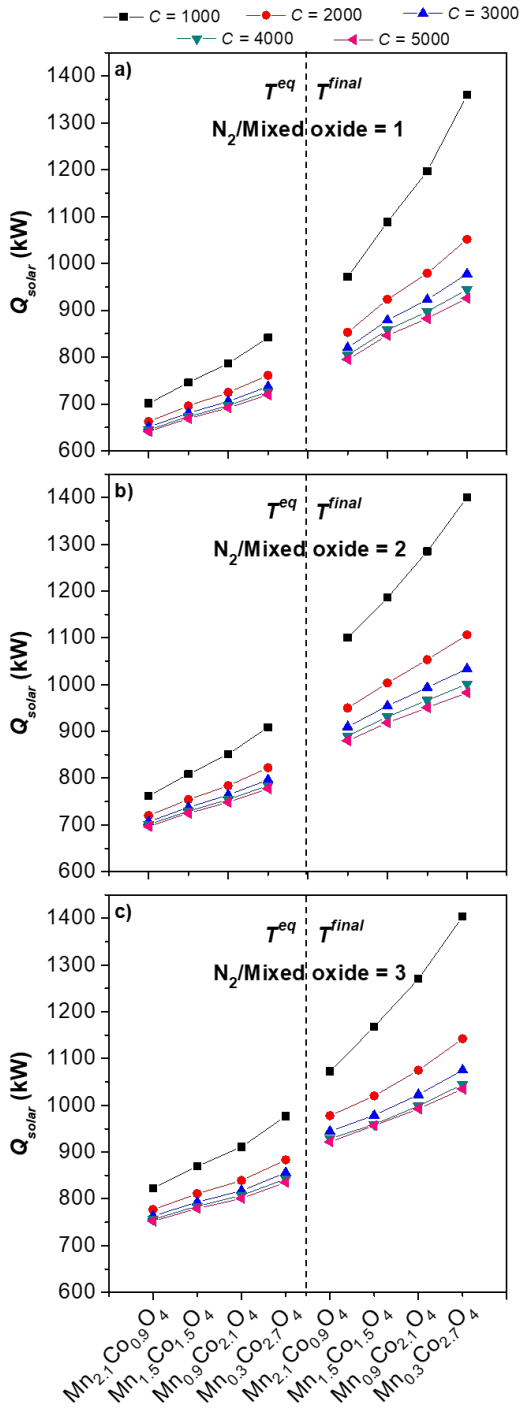

Figure 6. Evolution of solar heat input (Q_{solar}, equation 29) with the required temperature T^{eq} or T^{final} for a) N_2/mixed oxide = 1, b) N_2/mixed oxide = 2 and c) N_2/mixed oxide = 3.

The results indicate that the greater the proportion of N_2, the higher the solar heat input. For example, for the $Mn_{0.3}Co_{2.7}O_4$ material, the solar heat input increases from 841 to 978

kW when operating at T^{eq} and from 1361 to 1403 kW operating at T^{final} for a C = 1000 suns. This influence is more significant for a concentration ratio of 1000 suns because the optical losses in the concentrator are higher. In fact, the lower the value of C, the higher solar heat input is required. For example, for the $Mn_{0.3}Co_{2.7}O_4$ material, Q_{solar} goes from 922 to 1361 kW when C goes from 5000 to 1000 suns and at fixed N_2/mixed oxide molar ratio of 1. It can be concluded that $Mn_{2.1}Co_{0.9}O_4$ material requires the lowest solar heat input, so it is the most interesting material from a practical point of view.

3.3.3. Energy requirements NaOH recovery

To close the cycle, it is necessary to heat the NaOH solution exiting the hydrolysis unit in an evaporator to recover the NaOH. According to stoichiometry, H_2/H_2O ratio is 1, and consequently the water molar flow rate necessary for the production of 1 mol/s of H_2 should be also 1 mol/s. Based on that, Table 6 summarized the heat flow necessary for recovering NaOH calculated by equation 34 for stoichiometric conditions and also in excess of water.

Table 6. Required heat for NaOH recovery as a function of the water feed.

Water feed	**Stoichiometric ratio (SR)**	**2 × SR**	**3 × SR**
Heat (kW)	56	102	149

The required heat can be provided by electrical resistors which would imply extra energy consumption (as is indicated in equation 35) or using the energy recovered from other process streams. In order to evaluate the viability of this option, the Q_{cool} for the different units of the process were calculated, and the obtained values are summarized in Table 7 and Table 8.

Table 7. Heat recovered from the cooling units for a N_2 molar flow of 3 mol/s assuming $T_{reduction} = T^{eq}$ and $T_{oxidation} = T^{eq}$.

Material	Q_{cool} O_2+N_2 (kW)	Q_{cool} H_2+N_2 (kW)	Q_{cool} $Na_2Mn_{3-x}Co_xO_5$ (kW)	ΣQ_{cool} (kW)
$Mn_{0.3}Co_{2.7}O_4$	-82	-129	-336	-547
$Mn_{0.9}Co_{2.1}O_4$	-87	-122	-311	-520
$Mn_{1.5}Co_{1.5}O_4$	-91	-115	-291	-497
$Mn_{2.1}Co_{0.9}O_4$	-96	-108	-225	-429

Table 8. Heat recovered from the cooling units for a N_2 molar flow of 3 mol/s assuming $T_{reduction} = T^{final}$ and $T_{oxidation} = T^{final}$

Material	Q_{cool} O_2+N_2 (kW)	Q_{cool} H_2+N_2 (kW)	Q_{cool} $Na_2Mn_{3-x}Co_xO_5$ (kW)	ΣQ_{cool} (kW)
$Mn_{0.3}Co_{2.7}O_4$	-92	-157	-404	-653
$Mn_{0.9}Co_{2.1}O_4$	-96	-148	-376	-620
$Mn_{1.5}Co_{1.5}O_4$	-100	-141	-351	-592
$Mn_{2.1}Co_{0.9}O_4$	-105	-132	-274	-511

As it can be seen, the heat recovered is higher when the operating temperature is T_{final}. Comparing the values of ΣQ_{cool} from Tables 7 and 8 with the required heat in Table 6, it can be concluded that the energy requirements for the NaOH recovery can be supplied by the residual heat streams of the process. As no extra heat is necessary, equation 35 can be simplified to equation 39, and thus, equation 38 can be simplified to equation 40:

$$\eta_{solar\ to\ fuel} = \frac{n_{H_2} \cdot HHV_{H_2}}{Q_{solar}} \tag{39}$$

$$\varepsilon_{exergy} = \frac{0.65 \cdot n_{H_2} \cdot \psi_{ch,H_2}}{\psi_{solar}} \quad (40)$$

3.3.4. Solar to fuel and exergy efficiencies

The influence of the temperature in the energy efficiency, calculated as solar-to-fuel efficiency, and exergy efficiency for electricity production in a fuel cell, is shown in Figure 7 for a N_2/mixed oxide of 3. Increases in the temperature required for the process as the Mn content decreases, are associated to an increase in Q_{solar} caused by the lower η_{abs} at higher temperature and consequently to a reduction of both solar to fuel and exergy efficiencies. The results are highly dependent on the selection of temperature for the study (T^{eq} or T^{final}) revealing the evaluation of equilibrium composition of reactions involved in the process as a critical tool for energy and exergy calculations.

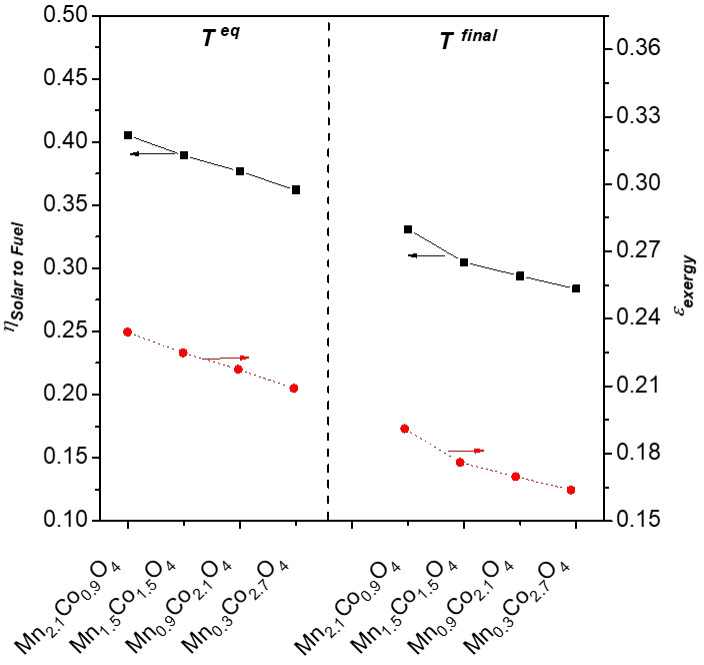

Figure 7. Influence of temperature in the solar to fuel efficiency and exergy efficiency according to: T^{eq} and T^{final}, for a N_2/mixed oxide = 3 and a value of C = 4000 suns.

It should be pointed out that the $Mn_{2.1}Co_{0.9}O_4$ mixed oxide can be considered as the most promising material from those evaluated in this work as it requires the lowest temperatures and presents the highest solar to fuel and exergy efficiencies. A further comparison between thermochemical water splitting for hydrogen production with this mixed oxide and Mn_2O_3/MnO without Co in the composition is shown in Figure 8 for C = 4000 suns. Data of energy and exergy efficiency in the graph come from data recently shown in literature [26]. It is remarkable that the $Mn_{2.1}Co_{0.9}O_4$/$Mn_{2.1}Co_{0.9}O_3$ thermochemical cycle shows energy and exergy efficiencies higher than those reported for Mn_2O_3/MnO when the operation temperature is T^{eq}. On the other hand, when the operational temperature is T^{final} these efficiencies are similar than those reported for the Mn_2O_3/MnO. These comparisons reinforce the proposal of the $Mn_{2.1}Co_{0.9}O_4$ as a promising material for hydrogen production by thermochemical water splitting.

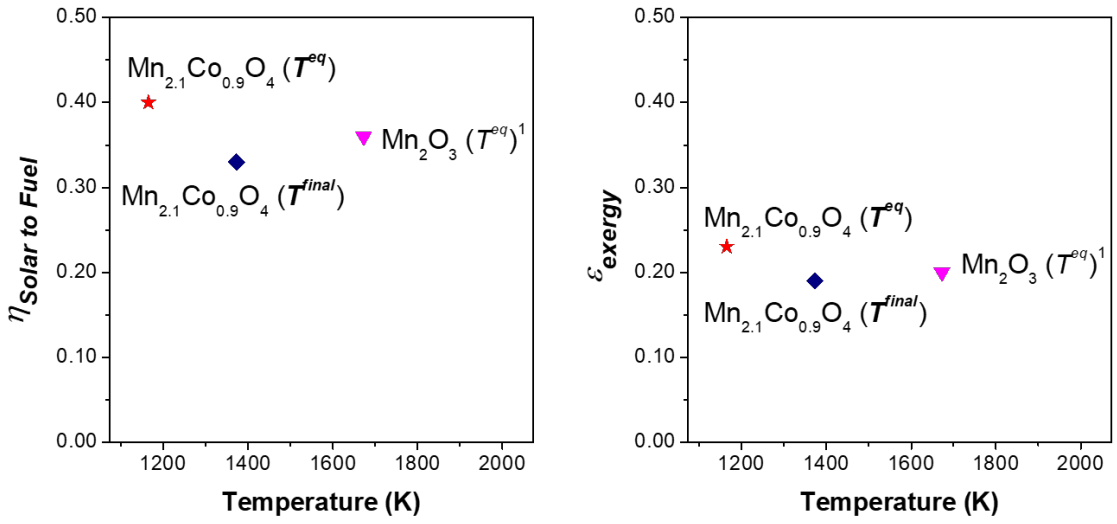

Figure 8. Comparison between pure and mixed metal-oxide thermochemical cycles for C= 4000 suns from: a) solar to fuel efficiency, and b) exergy efficiency values ([1]Data from [26] using T^{eq})

A recent review [31] showed a comparison of $\eta_{Solar\ to\ Fuel}$ and ε_{exergy} for different materials used in thermochemical cycles using C = 5000 suns (Figure 9). The calculation of the parameters found in literature and represented in Figure 9 follows a scheme and assumptions close to those used for the calculations of the $Mn_{2.1}Co_{0.9}O_4$ materials, but considering these deviations: i) in those works, the exergy for hydrogen in equation 39 (ψ_{ch,H_2}) is substituted by the Gibbs free energy for $\Delta G_{H_2+1/2O_2\rightarrow H_2O}$, with a value of 237.2 kJ/mol instead of 235.2 kJ/mol for the calculation; ii) solar exergy (ψ_{solar}) is simplified to Q_{solar}, instead of be calculated following equation 36. Nevertheless, it should be pointed out that, according to the values of T_0 and T_{sun}, equation 36 can be simplified to $0.93 \cdot Q_{solar}$. These deviations are really small, and consequently, the solar to fuel efficiencies and exergy efficiencies found in literature can be compared to those obtained by equation 39 and 40. The comparison with other thermochemical cycles reveals that $Mn_{2.1}Co_{0.9}O_4$ presents similar efficiencies but operating at quite lower temperatures and in a three step thermochemical cycle. Additionally, it is important to note that the results for these materials were estimated for the equilibrium temperature. On the other hand, $Mn_{2.1}Co_{0.9}O_4$ has similar efficiencies as other multiple-step thermochemical cycles, and even higher efficiencies than CeO_2, one of the most studied material for H_2 production by solar driven thermochemical cycles. These results confirm the $Mn_{2.1}Co_{0.9}O_4$ mixed oxide as a very promising material for a full scale H_2 production by solar driven thermochemical cycle.

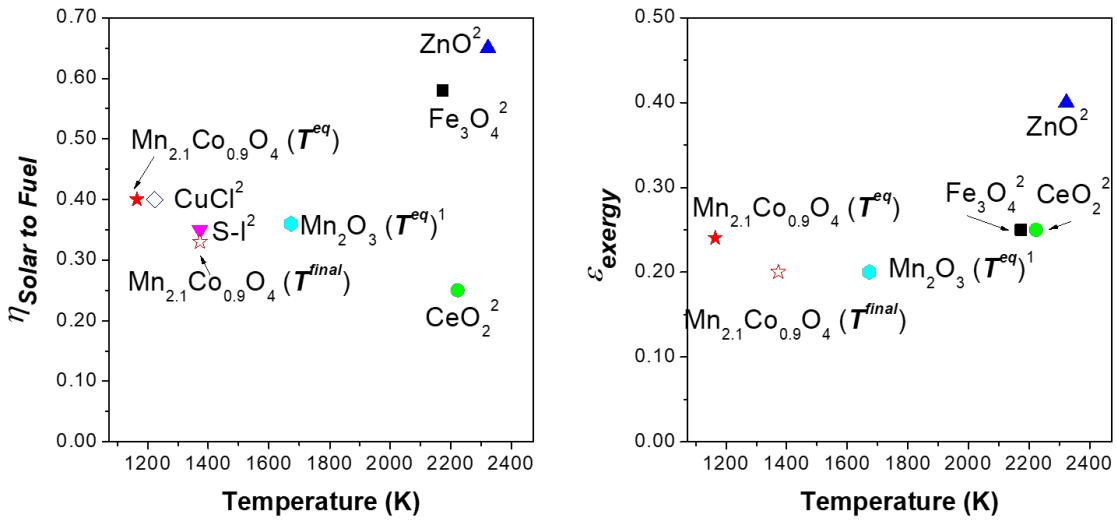

Figure 9. Comparison between metal-oxide thermochemical cycles for C= 5000 suns from: a) solar to fuel efficiency and b) exergy efficiency values ([1].Data from [26], [2].Data from [31]).

4. CONCLUSIONS

The thermodynamic study presented in this work shows that the thermal reduction of the manganese-cobalt mixed oxides can be carried out at temperatures ranging from 1048 to 1164 K, much lower than the 1723 K corresponding to the Mn_2O_3/MnO oxides. However, in contrast to most of the thermochemical cycles reported in the literature, the oxidation step with sodium hydroxide is only feasible at higher temperatures (1165-1325 K), being the limiting step of the cycle from a thermal point of view. These operational temperatures can be significantly decreased by using a higher flow of inert gas as carrier of the O_2 and H_2 liberated in the process, being compatible with conventional solar concentration technology. The material $Mn_{2.1}Co_{0.9}O_4$ exhibited the lowest operational temperatures and consequently the highest solar to fuel and exergy efficiencies, being the most promising material of all those evaluated. Finally, the comparison with other thermochemical cycles revealed that $Mn_{2.1}Co_{0.9}O_4$ presented similar or even higher efficiencies for hydrogen

production than the materials commonly reported in the literature, but working at quite lower temperatures.

ACKNOWLEDGEMENTS

The authors thank to "Comunidad de Madrid" and European Structural Funds for their financial support to ALCCONES project (S2013/MAE-2985) and ACES2030-CM project (S2018/EMT-4319).

5. REFERENCES

[1] F. Razi, I. Dincer, K. Gabriel. Thermal management of a new integrated copper-chlorine cycle for hydrogen production. *Energy Convers. Manag.,* 212 (2020) 112629-112641.

[2] A. Nixon, M. Ferrandon, M.H. Kaye, L. Trevani. Thermochemical Production of Hydrogen. *Advances in Hydrogen Production, Storage and Distribution Woodhead Publishing Limited*; (2011), pp. 263-280.

[3] M. Roeb, M. Neises, N. Monnerie, C. Friedemann, H. Simon, C. Sattler, M. Schmücker, R. Pitz-Paal. Materials-related aspects of thermochemical water and carbon dioxide splitting: A review. *Materials (Basel)*, 5 (11) (2012), pp. 2015-2054.

[4] F. Yılmaz, M. Tolga Balta. Energy and exergy analyses of hydrogen production step in boron based thermochemical cycle for hydrogen production. *Int. J. Hydrogen Energy*, 42 (2017), pp. 2485-2491.

[5] D. Graf, N. Monnerie, M. Roeb, M. Schmitz, C. Sattler. Economic comparison of solar hydrogen generation by means of thermochemical cycles and electrolysis. *Int. J. Hydrogen Energy,* 33 (2008), pp. 4511- 4519.

[6] R. Bhattacharyya, A. Misra, K.C. Sandeep. Photovoltaic solar energy conversion for hydrogen production by alkaline water electrolysis: conceptual design and analysis. *Energ. Convers. Manage.*, 133 (2017), pp. 1-13.

[7] A.O. Isenberg. Energy conversion via solid oxide electrolyte electrochemical cells at high temperature. *Solid State Ionics,* 3/4 (1981), pp. 431-437.

[8] C. Perkins, A.W. Weimer. Likely near-term solar-thermal water splitting technologies. *Int. J. Hydrogen Energy*, 29 (15) (2004), pp. 1587-1599.

[9] M. Roeb, N. Monnerie, A. Houaijia, D. Thomey, C. Sattler. Solar Thermal Water Splitting. *Renewable Hydrogen Technologies,* 4 (2013), pp. 63-86.

[10] C. Agrafiotis, M. Roeb, C. Sattler. A review on solar thermal syngas production via redox pair-based water/carbon dioxide splitting thermochemical cycles. *Renew Sustain Energy Rev*., 42 (2015), pp. 254-285.

[11] F. Safari, I. Dincer. A review and comparative evaluation of thermochemical water splitting cycles for hydrogen production. *Energy Convers. Manag.,* 205 (2020), pp. 112182-112199.

[12] T. Kodama, N. Gokon. Thermochemical cycles for high-temperature solar hydrogen production. *Chem. Rev*., 107 (10) (2007), pp. 4048–77.

[13] C.L Muhich, B.W. Evanko, K.C. Weston, P. Lichty, X. Liang, J. Martinek, C.B. Musgrave, A.W. Weimer. Efficient Generation of H_2 by Splitting Water with an Isothermal Redox Cycle. *Science,* 341 (6145) (2013), pp. 540-542.

[14] T. Abbasi T, S. A. Abbasi. "Renewable" hydrogen: Prospects and challenges. *Renew Sustain Energy Rev*., 15 (6) (2011), pp. 3034-3040.

[15] R.R. Bhosale, R.V. Shende, J.A. Puszynski. H_2 Generation from Thermochemical Water-Splitting Using Sol-Gel Derived Ni-Ferrite. *Journal of Power and Energy Engineering,* 4 (6) (2010), pp.27-38.

[16] J.R. Scheffe, A.H. McDaniel, M.D. Allendorf, A.W. Weimer. Kinetics and mechanism of solar-thermochemical H_2 production by oxidation of a cobalt ferrite–zirconia composite. *Energy Environ. Sci*., 6 (3) (2013), pp. 963-973.

[17] R.R. Bhosale, A. Kumar, P. Sutar. Thermodynamic analysis of solar driven SnO_2/SnO based thermochemical water splitting cycle. *Energy Convers. Manag.,* 134 (2017), pp. 226–235.

[18] N. Gokon, H. Murayama, J. Umeda, T. Hatamachi, T. Kodama. Monolitic zirconia-supported Fe_3O_4 for the two-step water-splitting thermochemical cycle at high thermal reduction temperatures of 1400-1600 °C, *Int. J. Hydrogen Energy,* 34 (2009), pp. 1208-1217.

[19] H. Ishihara, H. Kaneko, N. Hasegawa, Y. Tamaura. Two-step water-splitting at 1272-1623 K using yttria-stabilized zirconia-iron oxide solid solution via co-precipitation and solid-state reaction. *Energy,* 33 (2008), pp. 1788-1793.

[20] J. Miller, M. Allendorf, R. Diver, L. Evans, N. Seigel, J. Stuecker. Metal oxide composites and structures for ultra-high temperature solar thermochemical cycles. *J. Mater. Sci.,* 43 (2008), pp. 4714-4728.

[21] A. Haeussler, S. Abanades, J. Jouannaux, A. Julbe. Non-Stoichiometric Redox Active Perovskite Materials for Solar Thermochemical Fuel Production, *Catalysts, 8 (611)* (2018) pp.1-21.

[22] I. Vishnevetsky, M. Epstein. Hydrolysis rate of submicron Zn particles for solar H_2 synthesis. *Int. J. Hydrogen Energy,* 32 (2007), pp. 2791-2802.

[23] J. Marugán, J.A. Botas, R. Molina, C. Herradón. Study of the hydrogen production step of the Mn_2O_3/MnO thermochemical cycle. *Int. J. Hydrogen Energy,* 39 (10) (2014), pp. 5274-5282.

[24] J. Marugán, J.A. Botas, M. Martín, R. Molina, C. Herradón. Study of the the first

step of the Mn_2O_3/MnO thermochemical cycle for solar hydrogen production. *Int. J. Hydrogen Energy,* 37 (24) (2012), pp. 7017-7025.

[25] M. Lundberg, Model calculations on some feasible two-step water splitting processes, *Int. J. Hydrogen Energy,* 18 (1993), pp. 369–376.

[26] C. Herradón, R. Molina, J. Marugán, J.A. Botas. Experimental assessment of the cyclability of the Mn_2O_3/MnO thermochemical cycle for solar hydrogen production, *Int. J. Hydrogen Energy,* 44 (2019), pp. 91-100.

[27] M. Orfila, M. Linares, R. Molina, J.A. Botas, J. Marugán, R. Sanz. Thermochemical hydrogen production using manganese cobalt spinels as redox materials, *Int. J. Hydrogen Energy,* 42 (2017), pp. 13532-13543

[28] A. J. Carrillo, J. Moya, A. Bayón, P. Jana, V. A. de la Peña O'Shea, M. Romero, J. González-Aguilar, D. P. Serrano, P. Pizarro, J. M. Coronado. Thermochemical energy storage at high temperature via redox cycles of Mn and Co oxides: pure oxides versus mixed ones, *Sol. Energy Mater Sol Cells*, 123 (2014), pp. 43-57.

[29] J. Leitner, P. Chuchvalec, D. Sedmidubský, A. Strejc, P. Abrman. Estimation of heat capacities of solid mixed oxides. *Thermochim. Acta,* 395 (1-2) (2003), pp. 27–46.

[30] A. Bayón, V. A. De La Peña O'Shea, D. P. Serrano, J. M. Coronado. Influence of structural and morphological characteristics on the hydrogen production and sodium recovery in the NaOH-MnO thermochemical cycle. *Int. J. Hydrogen Energy,* 38 (30) (2013), pp. 13143–13152.

[31] D. Yadav and R. Banerjee, A Review of Solar Thermochemical Processes. *Renew. Sust. Energ. Rev.*, 54 (2016) pp.497-532.

[32] G.L. Schieber, E.B. Stechelb, A. Ambrosini, J.E. Miller, P.G. Loutzenhiser. H_2O splitting via a two-step solar thermoelectrolytic cycle based on non-stoichiometric

ceria redox reactions: Thermodynamic analysis. *Int. J. Hydrogen Energy,* 42 (30) (2017), pp. 18785-18793.

[33] R. Petela. Exergy of Undiluted Thermal Radiation. *Sol. Energy*, 74 (6) (2003), pp. 469–488.

[34] P.B. Kreider, H.H. Funke, K. Cuche, M. Schmidt, A. Steinfeld, A.W. Weimer, Manganese oxide based thermochemical hydrogen production cycle. *Int J Hydrogen Energy*, 36 (12) (2011), pp.7028-7037.

[35] J.E. Parrott, Choice of an Equivalent Black Body Solar Temperature. *Sol. Energy*, 51 (3) (1993), pp. 195-195.

[36] L.A. Weinstein, J. Loomis, B. Bhatia, D.M. Bierman, E.N. Wang, G. Chen. Concentrating Solar Power. *Chem. Rev.,* 115 (23) (2015), pp. 12797-12838.

[37] P. Charvin, S. Abanades, F. Lemort, G. Flamant. Hydrogen production by three-step solar thermochemical cycles using hydroxides and metal oxide systems. *Energ. Fuel.,* 21 (5) (2007), pp. 2919-2928.